

# 1 Genomic balancing selection is key to the invasive success of the fall armyworm

2 Sudeeptha Yainna<sup>1</sup>, Wee Tek Tay<sup>2</sup>, Estelle Fiteni<sup>1,3</sup>, Fabrice Legeai<sup>4,5</sup>, Anne-Laure Clamens<sup>6</sup>, Sylvie  
3 Gimenez<sup>1</sup>, Marie Frayssinet<sup>1</sup>, R Asokan<sup>7</sup>, CM Kalleshwaraswamy<sup>8</sup>, Sharanabasappa Deshmukh<sup>8</sup>,  
4 Robert L. Meagher, Jr.<sup>9</sup>, Carlos A. Blanco<sup>10</sup>, Pierre Silvie<sup>11,12,13</sup>, Thierry Brévault<sup>11,12</sup>, Anicet  
5 Dassou<sup>14</sup>, Gael J. Kergoat<sup>6</sup>, Thomas Walsh<sup>2</sup>, Karl Gordon<sup>2</sup>, Nicolas Nègre<sup>1</sup>, Emmanuelle  
6 d'Alençon<sup>1</sup>, Kiwoong Nam<sup>1\*</sup>

7 <sup>1</sup>DGIMI, Univ Montpellier, INRAE, Montpellier, France

8 <sup>2</sup>CSIRO, Black Mountain Laboratories, Canberra, Australia

9 <sup>3</sup>Université Claude Bernard Lyon 1, Lyon, France

10 <sup>4</sup>INRA, UMR-IGEPP, BioInformatics Platform for Agroecosystems Arthropods, Campus Beaulieu,  
11 Rennes, 35042, France

12 <sup>5</sup>INRIA, IRISA, GenOuest Core Facility, Campus de Beaulieu, Rennes, France

13 <sup>6</sup>CBGP, INRAE, CIRAD, IRD, Institut Agro, Univ Montpellier, Montpellier, France

14 <sup>7</sup>Division of Biotechnology, ICAR - Indian Institute of Horticultural Research, Bengaluru, India

15 <sup>8</sup>Department of Entomology, College of Agriculture, University of Agricultural and Horticultural  
16 Sciences, Shivamogga, India

17 <sup>9</sup>United States Department of Agriculture, Agricultural Research Service, Gainesville, Florida,  
18 U.S.A

19 <sup>10</sup>United States Department of Agriculture, Animal and Plant Health Inspection Service, Maryland,  
20 U.S.A.

21 <sup>11</sup>CIRAD, UPR AIDA, Montpellier, France

22 <sup>12</sup>AIDA, Univ. Montpellier, CIRAD, Montpellier, France

23 <sup>13</sup>IRD, UMR IPME, 34000, Montpellier, France

24 <sup>14</sup>ENSBBA, UNSTIM, Dassa, Benin

25

26 \*Correspondence: [ki-woong.nam@inrae.fr](mailto:ki-woong.nam@inrae.fr)

27 **Abstract**

28 **A successful biological invasion involves survival in a newly occupied environment. If a**  
29 **population bottleneck occurs during an invasion, the resulting depletion of genetic variants**  
30 **could cause increased inbreeding depression and decreased adaptive potential, which may**  
31 **result in a fitness reduction. How invasive populations survive in the newly occupied**  
32 **environment despite reduced heterozygosity and how, in many cases, they maintain moderate**  
33 **levels of heterozygosity are still contentious issues<sup>1</sup>. The Fall armyworm (FAW; Lepidoptera:**  
34 ***Spodoptera frugiperda*), a polyphagous pest, is native to the Western hemisphere. Its invasion**  
35 **in the Old World was first reported from West Africa in early 2016, and in less than four**  
36 **years, it swept sub-Saharan Africa and Asia, finally reaching Australia. We used population**  
37 **genomics approaches to investigate the factors that may explain the invasive success of the**  
38 **FAW. Here we show that genomic balancing selection played a key role in invasive success by**  
39 **restoring heterozygosity before the global invasion. We observe a drastic loss of mitochondrial**  
40 **polymorphism in invasive populations, whereas nuclear heterozygosity exhibits a mild**  
41 **reduction. The population from Benin in West Africa has the lowest length of linkage**  
42 **disequilibrium amongst all invasive and native populations despite its reduced population**  
43 **size. This result indicates that balancing selection increased heterozygosity by facilitating the**  
44 **admixture of invasive populations from distinct origins and that, once heterozygosity was**  
45 **sufficiently high, FAW started spreading globally in the Old World. As comparable**  
46 **heterozygosity levels between invasive and native populations are commonly observed<sup>1</sup>, we**  
47 **postulate that the restoration of heterozygosity through balancing selection could be**  
48 **widespread among successful cases of biological invasions.**

49 Keywords: adaptive evolution, Fall armyworm, invasive pests, population genomics, *Spodoptera*  
50 *frugiperda*

52 **Text**

53 A successful biological invasion involves the survival of an introduced population, which is  
54 typically associated with rapid adaptation processes in the newly occupied environment<sup>2,3</sup>. If a  
55 bottleneck occurs during an invasion as a result of the introduction of a small number of  
56 individuals, the invasive population may have a decreased fitness due to inbreeding depression  
57 because the level of heterozygosity is decreased<sup>4</sup>. Moreover, small populations may have a lower  
58 adaptive potential than large populations because of a lower population-scaled rate of mutation<sup>5-7</sup> or  
59 a lower number of existing genetic variants<sup>8</sup>, of which a proportion provides a beneficial effect for  
60 the survival in a new environment. The expectation that invasive populations have a reduced fitness  
61 appears to be contradictory with ample cases of invasive success, which has been often coined up as  
62 the ‘genetic paradox of biological invasion’<sup>9</sup>.

63 The occurrence of multiple introduction events has been proposed to be the solution to this paradox  
64 because genetic admixture among heterogeneous populations results in an increase in  
65 heterozygosity, which may decrease inbreeding depression and increase adaptive potential  
66 (reviewed in Estoup et al.<sup>1</sup>). However, the co-existence of allopatrically-originated individuals does  
67 not necessarily cause an increase in the level of heterozygosity because of the following two  
68 reasons. First, admixed individuals may have reduced fitness due to genetic incompatibilities  
69 between two haplotypes or strains. An established population is expected to have an optimal allelic  
70 combination through natural selection. Thus, admixed individuals between two established  
71 populations may have a substantial number of incompatible alleles, which decreases fitness. Indeed,  
72 genetic incompatibilities between populations are common in *Drosophila* fruit flies<sup>10</sup>. In addition,  
73 during the entire process of admixture, the stochastic effect of genetic drift may cause a substantial  
74 loss of variants if the initial number of invading individuals is small. In other words, a large  
75 effective population size is required to maintain variants from heterogeneous populations by  
76 overcoming genetic drift.

77 If selective advantages of admixed genotypes are sufficiently high to overcome the potential genetic  
78 incompatibilities in admixed individuals or to overcome genetic drift at the initial phase of  
79 admixture, then balancing selection may act in the way of facilitating admixture between different  
80 sets of genotypes from the different invasive origins. Therefore, it is tempting to hypothesize that  
81 invasive populations experience balancing selection, which restores heterozygosity during the  
82 lagging time between initial introductions to rapid range expansion.

83 The fall armyworm, *Spodoptera frugiperda* (J.E. Smith) (Lepidoptera: Noctuidae: Noctuinae), is  
84 one of the most infamous insect pests due to an extremely high-level of polyphagy (more than 353  
85 host-plants belonging to 76 plant families are reported<sup>11</sup>), high dispersal capacity and migratory  
86 behavior<sup>12</sup>, the rapid development of insecticide resistance<sup>13,14</sup>, including resistance to Bt proteins<sup>15-</sup>  
87 <sup>18</sup>, and occasional outbreaks<sup>19</sup>. The FAW is native to North and South America, and its presence in  
88 West Africa was first reported in 2016<sup>20</sup>. In the following years, the FAW spread across sub-  
89 Saharan Africa, followed by global detection in India, South East Asia, East Asia, Egypt, and  
90 Australia (<https://www.cabi.org/isc/fallarmyworm>). Invasive FAW larvae cause significant  
91 economic losses, especially on corn, with yield loss of corn production averaging 21%-53% in  
92 Africa<sup>21</sup>. The FAW consists of two strains, corn strain (sfC) and rice strain (sfR) (named after their  
93 supposedly preferred host-plants), which are observed sympatrically in all their native range<sup>22-24</sup>.  
94 Both strains are observed in invasive populations, while the relative proportion of the identified  
95 strains depends on their geographic location<sup>25-27</sup>. Tay et al., reported genomic signature of multiple  
96 introductions of FAW from Mississippi and South America to the Old World based on 870 unlinked  
97 single nucleotide variants (SNV)<sup>28</sup>. Potential multiple introductions and the recent explosive global  
98 invasion of the FAW makes this species an ideal model to test the potential effect of balancing  
99 selection in invasion success.

100 In this paper, we aim at testing the potential role of balancing selection in the global invasion of the  
101 FAW using population genomics. First, we identified genomic SNV (Single Nucleotide Variants)

102 from 177 samples in both native and invasive populations. Then, we inferred multiple origins of  
103 invasion, and tested balancing selection in the invasive population. Lastly, we identified adaptive  
104 evolution specific to invasive populations. We generated a new reference genome assembly from  
105 sfC using 30X PacBio Reads and Hi-C data<sup>29</sup>. The assembly size and N50 are 385 Mbp and 10.6  
106 Mbp, respectively. L90 is 26, which is close to the chromosome number in FAW (31), implying  
107 nearly chromosome-sized scaffolds in this assembly. BUSCO analysis<sup>30</sup> demonstrates that this  
108 assembly has the highest correctness among all published FAW genome assemblies (Table S1).

109 **The origin of invasion**

110 We performed whole genome sequencing from FAW samples collected in Benin (39 individuals),  
111 India (14), Mexico (26), Florida (24), French Guiana (3), and Guadeloupe (4) using novaseq 6000  
112 with 20X coverage on average (Fig. S1). This dataset was combined with resequencing data from  
113 populations collected in Mississippi (17) and Puerto Rico (15), which were used in our previous  
114 studies<sup>31,32</sup>. In addition, we had the opportunity of using resequencing data of Brazil (10), Malawi  
115 (16), and Uganda (7) from CSIRO<sup>28</sup>, Australia. Lastly, two individuals from China were also added  
116 to the dataset<sup>33</sup>. The resulting total number of individuals used in this study is 177 (99 from native  
117 populations and 78 from invasive populations). The mapping of genomes was performed against the  
118 reference assembly (Fig. S2), followed by variant calling using GATK<sup>34</sup>. After filtering, 27,117,672  
119 SNPs remained (see methods for more detail). We identified the strain from a maximum likelihood  
120 phylogenetic tree reconstructed from the full sequences of mitochondrial Cytochrome C Oxidase  
121 subunit I (COX1) gene, which is the universal barcode gene and also commonly used for FAW  
122 strain identification<sup>35</sup>. The COX1 phylogenetic tree shows high bootstrapping confidence scores for  
123 both sfC and sfR (bootstrap supporting value > 92%) (Fig. S3), with 99 and 78 and individuals  
124 being assigned to sfC and sfR, respectively. The invasive populations have 29 and 49 sfC and sfR  
125 individuals, respectively, and native populations have 70 and 29 sfC and sfR individuals,  
126 respectively.

127 A principal component analysis was performed from nuclear genome sequences to identify the  
128 origin of invasive populations. The first principal component shows three groups of individuals  
129 (Fig. 1A). The first group (sfR group) consists of sfR from the Caribbean, including Florida,  
130 Guadeloupe, and French Guiana, but also one individual from Mississippi. The second group (sfC  
131 group) consists of sfC from Mexico only. The third group (hybrid group) is found between the first  
132 and second groups along the first principal component, suggesting that this group was probably  
133 generated through intraspecific hybridization between sfC and sfR. The second principal component  
134 separates the hybrid group into native (Mississippi, Puerto Rico, Brazil, and Florida) and invasive  
135 (Benin, Malawi, Uganda, India, and China) populations. This result shows that hybrids were first  
136 generated in native populations and that these hybrids further invaded the Old World. This result is  
137 in line with previous studies, indicating that the vast majority of individuals of invasive populations  
138 are hybrids<sup>25-27</sup>. We also observed that both native hybrid populations and invasive populations  
139 exhibit reproductive barriers between sfC and sfR from genetic differentiation ( $F_{ST}$ ) with the  
140 statistical significance (Fig. S4).

141 The ancestry coefficient analysis<sup>36</sup> shows that invasive populations have homogeneous genomic  
142 sequences in a range of K values, while native populations show the heterogeneity except for sfC in  
143 Mexico (Fig. 1B). The BIO-NJ phylogenetic tree reconstructed from whole genome sequences  
144 exhibits 100% bootstrapping supports for sfC and sfR groups (Fig. 1C), in like with the PCA results  
145 (Fig. 1A). In addition, the tree also demonstrates that all invasive individuals belong to a single  
146 clade with bootstrap support of 100%, further highlighting the homogeneity of the invasive genomic  
147 background in all the locations of collections.

#### 148 **Reduction in genetic diversity during the invasion**

149 We then compared the genetic diversity between native hybrid populations and invasive  
150 populations. We assembled whole mitochondrial genomes, and we observed that we were able to  
151 extract high-quality full-length ND5 and COX1 sequences from all 177 individuals. In ND5, the

152 longest gene in the mitochondrial genome, sfC and sfR of the native hybrid populations have 26 and  
153 six polymorphic sites, respectively (Fig. 1D, left). However, sfC of the invasive populations has  
154 only one polymorphic site from 29 individuals (96.6% reduction), and sfR of the invasive  
155 populations has no polymorphic site from 43 individuals (100% reduction). We also compared  $\pi$   
156 (nucleotide diversity) between invasive populations and native hybrid populations from whole  
157 mitochondrial genomes. The nucleotide diversity of sfC and sfR was reduced during the invasion by  
158 78.32% ( $6.100 \times 10^{-4}$  and  $1.323 \times 10^{-4}$  for native hybrid populations and invasive populations,  
159 respectively) and by 78.45% ( $3.156 \times 10^{-4}$  and  $6.801 \times 10^{-5}$  for native hybrid populations and  
160 invasive populations, respectively), respectively. We identified eight and nine mitochondrial SNVs  
161 from sfC and sfR, respectively, but none of them was identified from native hybrid groups. This  
162 result implies that the observed SNVs in invasive populations were generated after the invasion,  
163 although we cannot exclude the possibility that these SNVs were derived from native hybrid  
164 populations that are not included in this study. The dramatic reduction in the mitochondrial genetic  
165 diversity, which was already shown in a previous study<sup>37</sup>, implies a severe genetic bottleneck during  
166 the invasion.

167 We further compared the number of nuclear biallelic heterozygous sites counted from each  
168 individual between native hybrid populations and invasive populations. We considered sites only if  
169 the genotype is determined from all 177 individuals to avoid potential statistical artifacts from  
170 missing data. Invasive populations have significantly lower numbers of heterozygous positions  
171 (Wilcoxon rank-sum test,  $p = 1.2 \times 10^{-14}$ ), while the average difference is only 12.71% (15,854.18  
172 and 18,162.53 for invasive populations and native hybrid populations, respectively, among  
173 412,404bp) (Fig. 1D, right). Interestingly, two individuals from India show almost the complete  
174 depletion of heterozygosity (B4 and B9), and one individual from Puerto Rico (PR19) has  
175 particularly high heterozygosity. The dramatic difference in the reduction of genetic diversity  
176 between mitochondrial and nuclear genomes suggests that the evolutionary forces reshaping  
177 polymorphism patterns is different between these two genomes.

178 Multiple introductions have been suggested to contribute to an increase in the heterozygosity of  
179 invasive populations. Thus, multiple origins of FAW might explain the moderate level of  
180 heterozygosity in invasive populations. However, this explanation alone cannot explain the  
181 difference between nuclear and mitochondrial patterns shown in Fig. 1D, because it is not realistic  
182 that the admixture increased only nuclear genetic diversity (which is heterozygosity in the case of  
183 diploid nuclear genomes) while mitochondrial genetic diversity remained unchanged.  
  
184 Instead, we postulate that genomic balancing selection increased nuclear heterozygosity in invasive  
185 FAW populations. In this scenario, (i) a severe bottleneck of an initially invasive population  
186 depleted heterozygosity, which caused inbreeding depression<sup>4</sup> (for example, reduced egg viability,  
187 increased mortality, and reduced life span as shown in inbred monarch butterflies<sup>38</sup>), (ii) this  
188 population had a lagging period where the nuclear heterozygosity gradually increased through  
189 genomic balancing selection, which facilitated admixture among populations with different invasive  
190 origins, while mitochondrial genetic diversity remained low, and (iii) when the heterozygosity has  
191 sufficiently increased to generate a stable population of the initially invasive population, the FAW  
192 was able to start its large scale invasion of the Old World.

### 193 **Genomic balancing selection**

194 To test the possibility of genomic balancing selection, we analyzed copy number variations (CNVs)  
195 to identify the origin of the invasive population with a higher resolution. As CNVs are much rarer  
196 than SNVs, we expected that CNVs have fewer noise signals from shared ancestral polymorphisms  
197 among multiple native populations to detect the invasive origin. We used CNVs only if minor allele  
198 frequency is higher than 0.2 to minimize false positives. The number of identified CNVs is 22,915.  
199 Ancestry coefficient analysis shows that, from a range of K values, invasive populations are divided  
200 into two groups (Fig. 2A). The first group includes Benin and India, and the second group includes  
201 Uganda, Malawi, and China. The first and the second groups have the same ancestry pattern from

202 sfC in Florida (Florida-sfC) and Brazil, respectively. This result demonstrates the occurrence of  
203 multiple introductions from Florida-sfC and Brazil.

204 The heterogeneous distribution of Florida-sfC-specific or Brazil-specific SNV among invasive  
205 individuals was tested. We counted the numbers of SNVs that are found only from Florida-sfC or  
206 Brazil for each individual in invasive populations, and these numbers were compared between the  
207 two invasive groups (Benin-India and Malawi-Uganda-China). Fig. 2B shows a nearly uniform  
208 distribution of SNV numbers specific to Florida-sfC-specific SNV across the entire invasive  
209 populations, and the SNV numbers were not significantly different between these two groups ( $p =$   
210 0.3502; 22,746.69 and 22,493.56 for Benin-India and Malawi-Uganda-China). The Malawi-  
211 Uganda-China group has a significantly higher number of Brazil-specific SNV than the Benin-India  
212 group ( $p = 6.519 \times 10^{-7}$ ; 11,934.20 and 12,484.84 for Benin-India and Malawi-Uganda-China,  
213 respectively), but with only a 4.61% difference between the two. These results show an almost  
214 uniform distribution of the numbers of Florida-sfC-specific or Brazil-specific SNVs among  
215 individuals in invasive populations, unlike what is found with CNVs.

216 Subsequently, we estimated to what extent the heterozygosity can be increased by admixture from  
217 SNVs that are absent in Brazil for each individual from Florida-sfC, assuming that these SNVs may  
218 increase the genetic diversity compared with a case that only Brazil is the only invading population.  
219 The numbers of these SNVs range from 656,760bp to 695,100bp (Fig. 2C). We also identified  
220 SNVs that are absent in Florida-sfC for each individual from Brazil. The numbers of these SNVs  
221 range from 378,299bp to 520,133bp. This result shows that the admixture between Florida-sfC and  
222 Brazil populations may increase the number of SNPs from 378kb to 695kb. The number of  
223 heterozygous positions in the invasive population is 1,629,133bp on average. Thus, the mixture  
224 might contribute to the heterozygous positions up to 42.67% of total invasive SNPs (695,100bp /  
225 1,629,133bp).

226 Then, we tested whether genomic balancing selection increases the level of heterozygosity by  
227 mixing genes between sfC-Florida and Brazil. In the presence of balancing selection, the length of  
228 the linkage disequilibrium is decreased because balancing selection has the same effect on the  
229 linkage disequilibrium with recombination hotspot<sup>39</sup>. Therefore, if invasive populations experienced  
230 genomic balancing selection, then these populations are expected to have shorter linkage  
231 disequilibrium than native populations. If balancing selection does not exist, invasive populations  
232 will have longer lengths of linkage disequilibrium than native populations because of smaller  
233 effective population sizes (i.e., smaller heterozygosity as shown in Fig. 1D). To test these  
234 alternative hypotheses, we compared the decay curve of linkage disequilibrium according to the  
235 distance from one locus to another for each strain of each population. We observed that the sfC and  
236 sfR from Benin had a faster decay of linkage disequilibrium than the other invasive populations as  
237 well as sfC-Florida or Brazil populations (Fig. 3A). When the decay of linkage disequilibrium was  
238 compared across all the native and invasive populations, sfC and sfR from Benin exhibit the fastest  
239 rate of decay (Fig S5). This result shows that the invasive population in Benin has a shorter linkage  
240 disequilibrium than native populations despite the smaller effective population size. This pattern is  
241 best explained by balancing selection that increases the genomic heterozygosity level of the  
242 population in Benin. Figure 3B shows a correlation of nucleotide diversity calculated from 100kb  
243 windows between invasive and native hybrid populations. The Pearson's correlation coefficient is  
244 very high ( $r = 0.992$ ,  $p < 2.2 \times 10^{-16}$ ), and outliers of this correlation are not observed. This pattern is  
245 in line with genomic balancing selection, rather than balancing selection affecting only a few loci.  
246 The shorter length of linkage disequilibrium in Benin is of particular interest because the FAW  
247 invasion was first reported on the Western coast of Africa, including Benin, Togo, Nigeria, and São  
248 Tomé and Príncipe<sup>20</sup>. Thus, we concluded that FAWs had increased heterozygosity by balancing  
249 selection in Benin (or other neighboring regions) and were able to spread eastward once their  
250 heterozygosity was sufficiently high.

251 **Testing alternate hypotheses**

252 An alternative explanation is that Florida-sfC-originated individuals co-existed with Brazil-  
253 originated individuals in Benin, while the admixture was incomplete compared with the other  
254 invasive populations. In this case, the heterogeneous genomic sequences among individuals in  
255 Benin may cause an underestimation of the length of linkage disequilibrium. We tested the  
256 heterogeneity in the population from Benin from CV (coefficient of variance) of Florida-sfC or  
257 Brazil derived variants (Fig. 2B) among invasive populations assuming that this heterogeneity  
258 among individuals increases the variance of Florida-sfC-specific or Brazil-specific SNV numbers.  
259 For the variants from Florida-sfC, CV was lowest in Benin (0.0194), followed by Malawi (0.0231),  
260 India (0.0241), and then Uganda (0.0535). For the variants from Brazil, CV was lowest in India  
261 (0.0184), followed by Benin (0.0202), Malawi (0.0332), and then Uganda (0.0527). This result  
262 shows that the population from Benin does not have a particularly high CV. Therefore, the  
263 heterogeneity of genomic sequences in Benin is not supported.

264 We then tested another alternative hypothesis that the level of heterozygosity in invasive  
265 populations is increased by interspecific hybridization with non-FAW species belonging to the same  
266 genus as there are several other *Spodoptera* species which are found in Africa and Asia including *S.*  
267 *littoralis* (Boisduval) in Africa, *S. mauritia* (Boisduval) and *S. litura* (Fabricius) in Asia, and *S.*  
268 *ciliatum* (Guenée) and *S. exigua* (Hübner) in Africa and Asia. In this case, the distribution of genetic  
269 differentiation is expected to show a bimodal distribution<sup>40</sup>, in which each mode represents the  
270 FAW and non-FAW species, respectively. The histogram of  $F_{ST}$  calculated from 100kb windows  
271 shows a unimodal distribution, in which 99.0% of windows have  $F_{ST}$  greater than zero (Fig. 4A).  
272 This distribution does not support inter-specific hybridization. We also tested the interspecific  
273 hybridization from the numbers of homozygous variant positions, which are expected to be  
274 increased by interspecific hybridization because, in this case, the non-FAW species have a longer  
275 phylogenetic distance from organism used to generate the reference genomes than the FAW in the  
276 native populations. In order to remove statistical artifacts, we considered positions only if genotypes  
277 are determined from all individuals. We observed that invasive populations have lower numbers of

278 homozygous variant positions than native populations (2954.295bp and 3170.527bp in total  
279 412,404bp for invasive and native populations, respectively;  $p = 0.005319$  Wilcoxon rank-sum test)  
280 (Fig. 4B), further showing that the interspecific hybridization between *Spodoptera* species is not  
281 supported.

282 **Identification of adaptive evolution in the invasive population**

283 We calculated the composite likelihood of selective sweeps<sup>41</sup> from invasive populations to identify  
284 positively selected genes that may contribute to adaptation in a new environment. The median value  
285 of the composite likelihood is 0.4350, and a locus is considered to be targeted by selective sweep if  
286 the composite likelihood is higher than 100, which was arbitrarily chosen. In total, we identified  
287 seven loci on three chromosomes as potential targets of selective sweeps (Fig. 5A). As the high  
288 composite likelihood of these loci might be generated by selective sweeps not specific to invasive  
289 populations or by background selection<sup>42</sup>, we calculated the composite likelihood from native  
290 hybrid populations as well. Four out of the seven loci do not exhibit outliers of the composite  
291 likelihood in native hybrid populations (Fig. S6). Therefore, we considered these four loci  
292 potentially targeted by selective sweeps specific to invasive populations. These four loci contain 36  
293 predicted protein-coding genes (Table S3), including 12 genes with unknown gene functions. We  
294 carefully underwent a manual curation of these genes to determine the function. The locus on  
295 chromosome 14 has CYP9A, which belongs to Cytochrome P450 gene family. This gene family  
296 plays a key role in detoxifying xenobiotics<sup>43</sup>, and CYP9A genes are overexpressed by plant  
297 allelochemicals and pesticides in FAW<sup>44</sup>. Therefore, positive selection on this gene might contribute  
298 to the adaptation to plants or pesticides in an invasive area. This locus also includes three copies of  
299 tubulin genes, implying that the cytoskeleton could be under positive selection as well.  
300 A locus on chromosome 29 includes a carboxylesterase gene, which may involve insecticides  
301 resistance<sup>45</sup>, and an ABC transporter homolog to mdr49, which protects organisms from cytotoxic  
302 compounds in *Drosophila melanogaster* Meigen<sup>46</sup>. Therefore, positive selection of these three genes

303 might mitigate environmental stresses in an invasive area. This locus also includes a kunitz-type  
304 serine protease inhibitor gene, which plays a role in the digestion of plants<sup>47</sup>. The gene encoding  
305 odorant receptor 13, which could be important for the selection of foraging or oviposition sites<sup>48</sup>, is  
306 also found from this loci. Invasive populations have reduced host plant ranges compared with native  
307 populations<sup>27,49</sup>. One of the possible explanations of this reduction is the genetic differentiation of  
308 the serine protease inhibitor gene or the odorant receptor gene by genetic linkage to selectively  
309 targeted carboxylesterase and mdr49 genes. In this explanation, the reduction of host-plant ranges is  
310 a by-product of the process of adaptive evolution to reduce environmental stress. However, the  
311 possibility of divergent selection on the host plant should be considered as well. Interestingly, this  
312 locus includes clk, a key circadian clock gene<sup>50</sup>. African populations of FAWs have an earlier  
313 mating time than American populations by three hours<sup>51</sup>. The genetic differentiation of clk could  
314 also be caused by genetic linkage to positively selected environmental stress genes or host-plant  
315 genes, while divergent selection on the circadian clock is also possible.

316 CNV exhibits two groups in the invasive population (Fig. 2A), unlike SNV. The first group  
317 includes Benin and India, and the second group includes China, Malawi, and Uganda. We tested the  
318 presence of positive selection by CNV that is specific to one or both groups in invasive populations.  
319  $F_{ST}$  calculated from CNV between Benin-India and China-Malawi-Uganda is 0.0397 (Fig. 5B).  $F_{ST}$   
320 calculated from SNV between these two groups is 0.00973, which represents only 24.5% of  $F_{ST}$   
321 from  $F_{ST}$  from CNV (0.00973/0.0397). In order to test if CNV having much higher  $F_{ST}$  than SNV is  
322 a general phenomenon, we also calculated  $F_{ST}$  between pairs among native hybrid populations, sfC  
323 group, and sfR group. The ratio of  $F_{ST}$  between these pairs from SNV to CNV ranges from 0.607 to  
324 2.36 (Fig. 5C), which is higher than the ratio of  $F_{ST}$  between Benin-India and China-Malawi-  
325 Uganda (0.245). Thus, we concluded that the  $F_{ST}$  calculated from CNV between Benin-India and  
326 China-Malawi-Uganda could be affected by positive selection on CNV. In total, six loci with CNV  
327 have almost complete genetic differentiation between the two groups ( $F_{ST} > 0.8$ ).  
328 We identified only one gene, Decaprenyl-diphosphate synthase subunit 2 (DDSS2), from these loci.

329 Most individuals in the China-Malawi-Uganda group have this gene as single-copy, while the  
330 Benin-India group lacks this gene in most individuals. In FAW, the DDSS gene is down-regulated  
331 by bat-induced stress<sup>52</sup>, and a region near Benin exhibits a hotspot for bat-species diversity<sup>53</sup>. Thus,  
332 the CNV of DDSS gene could possibly be a consequence of adaptation to local bat communities in  
333 West Africa (or India). More ecological studies are required to test the differential stress from  
334 predators across multiple invasive populations.

335 In this study, we showed that the restoration of the level of heterozygosity by genomic balancing  
336 selection is key to invasive success in FAW and that it likely enables its rapid global invasion of the  
337 Old World. We do not argue that invasive FAW in Western Africa obtained a new trait by adaptive  
338 evolution that increased invasiveness (e.g., Bridgehead Effects<sup>54,55</sup>). FAWs in native populations  
339 exhibit high migratory behavior, and invasive populations have probably equally high mobility as  
340 native populations. Instead, we argue here that the generation of a stable population in West Africa  
341 by genomic balancing selection played a key role in invasive success in FAW.

342 In addition, we do not argue that West Africa is the only initially invaded area. It is possible that the  
343 initial introduction of FAW might occur elsewhere in the Eastern Hemisphere<sup>28</sup>, while invasive  
344 FAW remained undetected due to their small population size. We argue here that genomic  
345 balancing selection is one of the causal evolutionary forces responsible for explosive population  
346 growth in West Africa by facilitating admixtures and that this population migrated eastward, as  
347 shown from the chronological order of detection of invasive FAW. If populations of FAW existed  
348 in the Eastern Hemisphere before the first detection in West Africa, potential gene flow among  
349 invasive populations could explain the different patterns of ancestry coefficients between CNV  
350 (Fig. 2A) and SNV (Fig. 1B) among invasive populations.

351 The majority of reported cases show that the reduction in heterozygosity is mild (e.g., < 20%) in a  
352 wide range of taxa<sup>1</sup>. Therefore, it could be postulated that balancing selection may play a key role in  
353 the invasive success of a large range of organisms. Future studies should involve population  
354 genomics analysis in other invasive taxa to test this possibility. This study also highlights the

355 importance of rapid and vigorous pest control during the early phase of the invasion, as emphasized  
356 by many researchers, before heterozygosity is sufficiently increased to generate a stable population  
357 by genomic balancing selection. For an early eradication, early monitoring of pest species is  
358 mandatory, and a small number of individuals should not be overlooked, like the case of the Asian  
359 hornet (*Vespa velutina* Lepeletier) that started from a small invasive population which then went on  
360 to rapidly colonize large areas of Western Europe<sup>56</sup>.

361 **Methods**

362 **Genome assembly**

363 We performed the mapping of Illumina reads (~80X)<sup>57</sup> against an assembly, which was generated  
364 from 30X PacBio Reads in our previous study<sup>32</sup>, using SMALT<sup>58</sup>, and potential errors in the  
365 assemblies were identified using reapr<sup>59</sup>. If an error is found over a gap, the scaffold was broken  
366 into two using the same software to remove potential structural errors in the assembly. The broken  
367 assemblies were concatenated using SALSA2<sup>60</sup> or 3D-DNA<sup>61</sup>, followed by gap filling with the 80X  
368 Illumina reads using SOAP-denovo2 Gap-Closer<sup>62</sup> and with the PacBio reads using LR\_GapCloser  
369 v1.1<sup>63</sup>. We observed that 3D-DNA generated a slightly more correct assembly than SALSA2 from  
370 BUSCO analysis (Table S1). Thus, the assembly from 3D-DNA was used in this study. Gene  
371 annotation was transferred from the previously generated assemblies to current assembly using  
372 RATT<sup>64</sup>.

373

374 **Resequencing Data**

375 FAW larvae were collected from Wagou and Gando Villages in Benin (2017), from Citra and  
376 Jacksonville in Florida (2015), from Texcoco in Mexico (2009), from French Guiana (1992), and  
377 from Petit-Bourg and Port-Louis in Guadeloupe (2013). We obtained gDNA from India, which was

378 used by Sharanabasappa et al<sup>65</sup>. Genomic DNA was extracted using the Wizard Genomic DNA kit  
379 or the Qiagen Dneasy blood and tissues kit. Libraries for whole genome resequencing were  
380 constructed from 1.0µg DNA per sample using NEBNext DNA Library Prep Kit. Novaseq 6000  
381 with ~20X coverage was used to perform whole genome resequencing with 150bp paired-end and  
382 300bp insert length. Then, we combined the resequencing data from Puerto Rico and Mississippi,  
383 which were generated for our previous studies (Hiseq 2500, Hiseq 4000, and Novaseq 6000)<sup>31,32</sup>, as  
384 well as the resequencing data of Brazil, Malawi, and Uganda from CSIRO (Novaseq 6000, 150bp  
385 paired-end sequencing)<sup>28</sup>. Lastly, resequencing data from China<sup>33</sup> was also combined with the  
386 dataset. Adapter sequences were removed using adapterremoval<sup>66</sup>. Then, we performed mapping of  
387 reads against the reference genome using bowtie2<sup>67</sup>. Then, we performed a variant calling using  
388 GATK<sup>34</sup>. Filtering was performed if QD is lower than 2.0, or FS is higher than 60.0, or MQ is  
389 lower than 40.0, or MQRankSum is lower than -12.5, or ReadPosRankSum is lower than -8.0.  
390 CNVs were identified using CNVCaller<sup>68</sup>. We discarded all CNVs unless minor allele frequency is  
391 higher than 0.2 to reduce false positives.

392 **Phylogenetic analysis**

393 To identify strains, we mapped the Illumina reads against mitochondrial genomes (NCBI:  
394 KM362176) using bowtie2<sup>67</sup>, followed by extracting mitochondrial reads using samtools<sup>69</sup>.  
395 Mitochondrial genomes were assembled using MitoZ<sup>70</sup>, and COX1 sequences were identified.  
396 These COX1 sequences were aligned together with a COX1 sequence from a specimen of another  
397 *Spodoptera* species, *S. exigua* (NCBI ID, JX316220), using MUSCLE<sup>71</sup>, and a maximum  
398 likelihood phylogenetic tree was reconstructed using PhyML<sup>72</sup>. The phylogenetic tree was  
399 visualized using iTOL<sup>73</sup>.  
400 We calculated the nuclear genetic distance between each pair of individuals from the difference in  
401 allele frequency at biallelic sites in which genotypes are determined from all individuals using  
402 VCFphylo (<https://github.com/kiwoong-nam/VCFPhylo>). Transversional variants were weighted to

403 two. Then, a bootstrapping distance matrix was generated with 1,000 replications, and we generated  
404 BIO-NJ trees for each matrix using FastME<sup>74</sup>. Then, a consensus tree was made using consense in  
405 Phylip package<sup>75</sup>, and the tree was visualized using iTOL<sup>73</sup>.

406 **Population genomics analysis**

407 The principal component analysis was performed using plink<sup>76</sup>. We used admixture<sup>36</sup> for the  
408 ancestry coefficient analysis. Weir and Cockerham's  $F_{ST}$ <sup>77</sup> was calculated using VCFtools<sup>78</sup>.  
409 Potential targets of selective sweeps were identified using SweeD<sup>41</sup>. The number of the grid is 1,000  
410 per chromosome. If a locus has the composite likelihood of selective sweeps higher than 100, we  
411 considered that this locus was targeted by a selective sweep. The decay curves of linkage  
412 disequilibrium were generated using PopLDdecay<sup>79</sup>. To identify mitochondrial SNVs, a  
413 mitochondrial VCF was generated from the bam files, which was made to identify strains (see  
414 above), using GATK<sup>34</sup>.

415 **References**

1. Estoup, A. *et al.* Is there a genetic paradox of biological invasion? *Annu. Rev. Ecol. Evol. Syst.* **47**, 51–72 (2016).
2. Lee, C. E. Evolutionary genetics of invasive species. *Trends Ecol. Evol.* **17**, 386–391 (2002).
3. Whitney, K. D. & Gabler, C. A. Rapid evolution in introduced species, ‘invasive traits’ and recipient communities: challenges for predicting invasive potential. *Divers. Distrib.* **14**, 569–580 (2008).
4. Charlesworth, D. & Willis, J. H. The genetics of inbreeding depression. *Nat. Rev. Genet.* **10**, 783–796 (2009).
5. Lanfear, R., Kokko, H. & Eyre-Walker, A. Population size and the rate of evolution. *Trends Ecol. Evol.* **29**, 33–41 (2014).
6. Grossman, S. R. *et al.* Identifying recent adaptations in large-scale genomic data. *Cell* **152**, 703–713 (2013).
7. Nam, K. *et al.* Evidence that the rate of strong selective sweeps increases with population size in the great apes. *Proc. Natl. Acad. Sci.* **114**, 1613–1618 (2017).
8. Hermisson, J. & Pennings, P. S. Soft Sweeps: Molecular population genetics of adaptation from standing genetic variation. *Genetics* **169**, 2335–2352 (2005).
9. Allendorf, F. W. & Lundquist, L. L. Introduction: population biology, evolution, and control of invasive species. *Conserv. Biol.* **17**, 24–30 (2003).
10. Corbett-Detig, R. B., Zhou, J., Clark, A. G., Hartl, D. L. & Ayroles, J. F. Genetic incompatibilities are widespread within species. *Nature* **504**, 135–137 (2013).
11. Montezano, D. G. *et al.* Host plants of *Spodoptera frugiperda* (Lepidoptera: Noctuidae) in the Americas. *Afr. Entomol.* **26**, 286–300 (2018).
12. Westbrook, J. K., Nagoshi, R. N., Meagher, R. L., Fleischer, S. J. & Jairam, S. Modeling seasonal migration of fall armyworm moths. *Int. J. Biometeorol.* **60**, 255–267 (2016).
13. Gutiérrez-Moreno, R. *et al.* Field-Evolved Resistance of the Fall Armyworm (Lepidoptera: Noctuidae) to Synthetic Insecticides in Puerto Rico and Mexico. *J. Econ. Entomol.* **112**, 792–802 (2019).
14. Mota-Sánchez, D. & John C., W. Arthropod Pesticide Resistance Database.  
<https://www.pesticideresistance.org/index.php>.
15. Storer, N. P. *et al.* Discovery and Characterization of Field Resistance to Bt Maize: *Spodoptera*

*frugiperda* (Lepidoptera: Noctuidae) in Puerto Rico. *J. Econ. Entomol.* **103**, 1031–1038 (2010).

16. Jakka, S. R. K. *et al.* Field-Evolved Mode 1 Resistance of the Fall Armyworm to Transgenic Cry1Fa-Expressing Corn Associated with Reduced Cry1Fa Toxin Binding and Midgut Alkaline Phosphatase Expression. *Appl. Environ. Microbiol.* **82**, 1023–1034 (2016).

17. Omoto, C. *et al.* Field-evolved resistance to Cry1Ab maize by *Spodoptera frugiperda* in Brazil. *Pest Manag. Sci.* **72**, 1727–1736 (2016).

18. Chandrasena, D. I. *et al.* Characterization of field-evolved resistance to *Bacillus thuringiensis*-derived Cry1F δ-endotoxin in *Spodoptera frugiperda* populations from Argentina. *Pest Manag. Sci.* **74**, 746–754 (2018).

19. Sparks, A. N. A review of the biology of the fall armyworm. *Fla. Entomol.* 82–87 (1979).

20. Goergen, G., Kumar, P. L., Sankung, S. B., Togola, A. & Tamò, M. First report of outbreaks of the fall armyworm *Spodoptera frugiperda* (J E Smith) (Lepidoptera, Noctuidae), a new alien invasive pest in west and central Africa. *PLOS ONE* **11**, e0165632 (2016).

21. Day, R. *et al.* Fall Armyworm: impacts and implications for Africa. *Outlooks Pest Manag.* **28**, 196–201 (2017).

22. Pashley, D. P. Host-associated genetic differentiation in fall armyworm (Lepidoptera: Noctuidae): a sibling species complex? *Ann. Entomol. Soc. Am.* **79**, 898–904 (1986).

23. Pashley, D. P. & Martin, J. A. Reproductive incompatibility between host strains of the fall armyworm (Lepidoptera: Noctuidae). *Ann. Entomol. Soc. Am.* **80**, 731–733 (1987).

24. Dumas, P. *et al.* *Spodoptera frugiperda* (Lepidoptera: Noctuidae) host-plant variants: two host strains or two distinct species? *Genetica* **143**, 305–316 (2015).

25. Zhang, L. *et al.* High-depth resequencing reveals hybrid population and insecticide resistance characteristics of fall armyworm (*Spodoptera frugiperda*) invading China. *bioRxiv* 813154 (2019) doi:10.1101/813154.

26. Nagoshi, R. N. *et al.* Comparative molecular analyses of invasive fall armyworm in Togo reveal strong similarities to populations from the eastern United States and the Greater Antilles. *PLoS ONE* **12**, (2017).

27. Nagoshi, R. N., Goergen, G., Plessis, H. D., van den Berg, J. & Meagher, R. Genetic comparisons of fall armyworm populations from 11 countries spanning sub-Saharan Africa provide insights into strain composition and migratory behaviors. *Sci. Rep.* **9**, 8311 (2019).

28. Tay, W. T. *et al.* Whole genome sequencing of global *Spodoptera frugiperda* populations: evidence for complex, multiple introductions across the Old World. *bioRxiv* 2020.06.12.147660 (2020) doi:10.1101/2020.06.12.147660.
29. Lieberman-Aiden, E. *et al.* Comprehensive mapping of long-range interactions reveals folding principles of the human genome. *Science* **326**, 289–293 (2009).
30. Simão, F. A., Waterhouse, R. M., Ioannidis, P., Kriventseva, E. V. & Zdobnov, E. M. BUSCO: assessing genome assembly and annotation completeness with single-copy orthologs. *Bioinformatics* **31**, 3210–3212 (2015).
31. Nam, K. *et al.* Adaptation by copy number variation increases insecticide resistance in fall armyworms. *bioRxiv* 812958 (2019) doi:10.1101/812958.
32. Nam, K. *et al.* Divergent selection causes whole genome differentiation without physical linkage among the targets in *Spodoptera frugiperda* (Noctuidae). *bioRxiv* 452870 (2018) doi:10.1101/452870.
33. Liu, H. *et al.* Chromosome level draft genomes of the fall armyworm, *Spodoptera frugiperda* (Lepidoptera: Noctuidae), an alien invasive pest in China. *bioRxiv* 671560 (2019) doi:10.1101/671560.
34. McKenna, A. *et al.* The Genome Analysis Toolkit: A MapReduce framework for analyzing next-generation DNA sequencing data. *Genome Res.* **20**, 1297–1303 (2010).
35. Lu, Y. & Adang, M. J. Distinguishing fall armyworm (Lepidoptera: Noctuidae) strains using a diagnostic mitochondrial DNA marker. *Fla. Entomol.* **79**, 48–55 (1996).
36. Alexander, D. H., Novembre, J. & Lange, K. Fast model-based estimation of ancestry in unrelated individuals. *Genome Res.* **19**, 1655–1664 (2009).
37. Nagoshi, R. N. *et al.* Analysis of strain distribution, migratory potential, and invasion history of fall armyworm populations in northern Sub-Saharan Africa. *Sci. Rep.* **8**, 3710 (2018).
38. Mongue, A. J., Tsai, M. V., Wayne, M. L. & de Roode, J. C. Inbreeding depression in monarch butterflies. *J. Insect Conserv.* **20**, 477–483 (2016).
39. DeGiorgio, M., Lohmueller, K. E. & Nielsen, R. A model-based approach for identifying signatures of ancient balancing selection in genetic data. *PLoS Genet.* **10**, e1004561 (2014).
40. Anderson, C. J. *et al.* Hybridization and gene flow in the mega-pest lineage of moth, *Helicoverpa*. *Proc. Natl. Acad. Sci.* **115**, 5034–5039 (2018).
41. Pavlidis, P., Živković, D., Stamatakis, A. & Alachiotis, N. SweeD: likelihood-based detection of selective sweeps in thousands of genomes. *Mol. Biol. Evol.* **30**, 2224–2234 (2013).

42. Charlesworth, B., Morgan, M. T. & Charlesworth, D. The effect of deleterious mutations on neutral molecular variation. *Genetics* **134**, 1289–1303 (1993).
43. McDonnell, A. M. & Dang, C. H. Basic review of the cytochrome P450 system. *J. Adv. Pract. Oncol.* **4**, 263–268 (2013).
44. Giraudo, M. *et al.* Cytochrome P450s from the fall armyworm (*Spodoptera frugiperda*): responses to plant allelochemicals and pesticides. *Insect Mol. Biol.* **24**, 115–128 (2015).
45. Cui, F. *et al.* Carboxylesterase-mediated insecticide resistance: Quantitative increase induces broader metabolic resistance than qualitative change. *Pestic. Biochem. Physiol.* **121**, 88–96 (2015).
46. Tapadia, M. G. & Lakhota, S. C. Expression of mdr49 and mdr65 multidrug resistance genes in larval tissues of *Drosophila melanogaster* under normal and stress conditions. *Cell Stress Chaperones* **10**, 7–11 (2005).
47. Lin, H. *et al.* Characterization and expression profiling of serine protease inhibitors in the diamondback moth, *Plutella xylostella* (Lepidoptera: Plutellidae). *BMC Genomics* **18**, 162 (2017).
48. de Fouchier, A. *et al.* Functional evolution of Lepidoptera olfactory receptors revealed by deorphanization of a moth repertoire. *Nat. Commun.* **8**, 15709 (2017).
49. Goergen, G., Kumar, P. L., Sankung, S. B., Togola, A. & Tamò, M. First report of outbreaks of the Fall Armyworm *Spodoptera frugiperda* (J E Smith) (Lepidoptera, Noctuidae), a new alien invasive pest in West and Central Africa. *PLOS ONE* **11**, e0165632 (2016).
50. Tataroglu, O. & Emery, P. The molecular ticks of the *Drosophila* circadian clock. *Curr. Opin. Insect Sci.* **7**, 51–57 (2015).
51. Haenniger, S. *et al.* Sexual communication of *Spodoptera frugiperda* from West Africa: Adaptation of an invasive species and implications for pest management. *Sci. Rep.* **10**, 2892 (2020).
52. Cinel, S. D. & Taylor, S. J. Prolonged bat call exposure induces a broad transcriptional response in the male fall armyworm (*Spodoptera frugiperda*; Lepidoptera: Noctuidae) brain. *Front. Behav. Neurosci.* **13**, (2019).
53. Herkt, K. M. B., Barnikel, G., Skidmore, A. K. & Fahr, J. A high-resolution model of bat diversity and endemism for continental Africa. *Ecol. Model.* **320**, 9–28 (2016).
54. Lombaert, E. *et al.* Bridgehead effect in the worldwide invasion of the biocontrol Harlequin ladybird. *PLoS ONE* **5**, e9743 (2010).
55. Bertelsmeier, C. & Keller, L. Bridgehead effects and role of adaptive evolution in invasive populations.

*Trends Ecol. Evol.* **33**, 527–534 (2018).

- 56 Rortais, A. *et al.* A new enemy of honeybees in Europe: the Asian Hornet, *Vespa velutina*. (2010).
57. Gouin, A. *et al.* Two genomes of highly polyphagous lepidopteran pests (*Spodoptera frugiperda*, Noctuidae) with different host-plant ranges. *Sci. Rep.* **7**, 11816 (2017).
58. Sanger Institute. SMALT (<https://www.sanger.ac.uk/tool/smalt-0/>).
59. Hunt, M. *et al.* REAPR: a universal tool for genome assembly evaluation. *Genome Biol.* **14**, R47 (2013).
60. Ghurye, J. *et al.* Integrating Hi-C links with assembly graphs for chromosome-scale assembly. *PLOS Comput. Biol.* **15**, e1007273 (2019).
61. Dudchenko, O. *et al.* De novo assembly of the *Aedes aegypti* genome using Hi-C yields chromosome-length scaffolds. *Science* **356**, 92–95 (2017).
62. Luo, R. *et al.* Erratum: SOAPdenovo2: an empirically improved memory-efficient short-read de novo assembler. *GigaScience* **4**, 30 (2015).
63. Xu, G.-C. *et al.* LR\_Gapcloser: a tiling path-based gap closer that uses long reads to complete genome assembly. *GigaScience* **8**, (2018).
64. Otto, T. D., Dillon, G. P., Degrave, W. S. & Berriman, M. RATT: Rapid Annotation Transfer Tool. *Nucleic Acids Res.* **39**, e57 (2011).
65. Sharanabasappa, et al. First report of the fall armyworm, *Spodoptera frugiperda* (J E Smith) (Lepidoptera: Noctuidae), an alien invasive pest on maize in India. *Pest Manag. Hortic. Ecosyst.* **24**, 23–29 (2018).
66. Schubert, M., Lindgreen, S. & Orlando, L. AdapterRemoval v2: rapid adapter trimming, identification, and read merging. *BMC Res. Notes* **9**, 88 (2016).
67. Langmead, B. & Salzberg, S. L. Fast gapped-read alignment with Bowtie 2. *Nat. Methods* **9**, 357–359 (2012).
68. Wang, X. *et al.* CNVcaller: highly efficient and widely applicable software for detecting copy number variations in large populations. *GigaScience* **6**, (2017).
69. Li, H. *et al.* The Sequence Alignment/Map format and SAMtools. *Bioinformatics* **25**, 2078–2079 (2009).
70. Meng, G., Li, Y., Yang, C. & Liu, S. MitoZ: a toolkit for animal mitochondrial genome assembly, annotation and visualization. *Nucleic Acids Res.* **47**, e63–e63 (2019).
71. Edgar, R. C. MUSCLE: multiple sequence alignment with high accuracy and high throughput. *Nucleic Acids Res.* **32**, 1792–1797 (2004).

72. Guindon, S. *et al.* New algorithms and methods to estimate maximum-likelihood phylogenies: assessing the performance of PhyML 3.0. *Syst. Biol.* **59**, 307–321 (2010).
73. Letunic, I. & Bork, P. Interactive Tree Of Life (iTOL) v4: recent updates and new developments. *Nucleic Acids Res.* **47**, W256–W259 (2019).
74. Lefort, V., Desper, R. & Gascuel, O. FastME 2.0: A comprehensive, accurate, and fast distance-based phylogeny inference program. *Mol. Biol. Evol.* **32**, 2798–2800 (2015).
75. Plotree, D. & Plotgram, D. PHYLIP-phylogeny inference package (version 3.2). *cladistics* **5**, 163–166 (1989).
76. Rentería, M. E., Cortes, A. & Medland, S. E. Using PLINK for genome-wide association studies (GWAS) and data analysis. in *Genome-Wide Association Studies and Genomic Prediction* (eds. Gondro, C., van der Werf, J. & Hayes, B.) 193–213 (Humana Press, 2013). doi:10.1007/978-1-62703-447-0\_8.
77. Weir, B. S. & Cockerham, C. C. Estimating F-statistics for the analysis of population structure. *Evolution* **38**, 1358–1370 (1984).
78. Danecek, P. *et al.* The variant call format and VCFtools. *Bioinformatics* **27**, 2156–2158 (2011).
79. Zhang, C., Dong, S.-S., Xu, J.-Y., He, W.-M. & Yang, T.-L. PopLDdecay: a fast and effective tool for linkage disequilibrium decay analysis based on variant call format files. *Bioinformatics* **35**, 1786–1788 (2019).

417

418 **End notes**

419 **Acknowledgements**

420 This work (ID 1702-018, given to KN) was publicly funded through ANR (the French National  
421 Research Agency) under the "Investissements d'avenir" programme with the reference ANR-10-  
422 LABX-001-01 Labex Agro and coordinated by Agropolis Fondation under the frame of I-SITE  
423 MUSE (ANR-16-IDEX-0006). In addition, a grant from the department of Santé des Plantes et  
424 Environnement at Institut national de la recherche agronomique for KN (adaptivesv). This work  
425 was also financially supported by EUPHRESCO (FAW-spedcom, given to Anne-Nathalie Volkoff)  
426 and by CSIRO Health & biosecurity (given to WTT, TW, and KG). SY was supported by a  
427 CIRAD-INRAE PhD fellowship.

428

429 **Author Contributions**

430 FL generated reference genome assembly. WTT, MF, SD, RA, CMK, RLMJ, CAB, PS, TB, AD,  
431 TW, KG, and NN provided samples for whole genome resequencing. EF, ANC, SG, and GJK  
432 prepared samples. EF performed variant calling. SY and KN performed analysis. NN and EA  
433 performed gene annotation. SY and KN wrote manuscript. KN involved in planning and supervised  
434 the work.

435

436 **Competing interests**

437 The authors declare no competing interests.

438

439 **Additional Information**

440 The raw reads of these samples are available from NCBI SRA (PRJNA639296 for samples from  
441 Florida and PRJNA639295 for the rest of the samples). The reference genome assembly used in this  
442 study is available at BIPAA ([https://bipaa.genouest.org/sp/spodoptera\\_frugiperda](https://bipaa.genouest.org/sp/spodoptera_frugiperda)).

443 Supplementary Information is available for this paper. We declare a full code availability upon

444 request.

445 **Figure legends**

446

447 **Figure 1. Population structure of fall armyworms.** A. Principal component analysis. B. Ancestry  
448 coefficient analysis with varying K values. C. BIO-NJ phylogenetic tree was reconstructed from the  
449 allelic differentiation between a pair of individuals with 1,000 replication of bootstrapping. The  
450 circles on the branches show bootstrapping support higher than 90%. D. (left) The numbers of SNPs  
451 on the mitochondrial ND5 gene in sfC and sfR. The numbers above the bars indicate the number of  
452 sequences. (right) The number of heterozygous positions counted from positions of which  
453 genotypes are determined from all individuals. The error bars indicate 95% confidence intervals  
454 calculated from 1,000 times of bootstrapping replications in the way of resampling from 100kb  
455 windows.

456

457 **Figure 2. Multiple introduction of invasive fall armyworm** A. Ancestry coefficient analysis of  
458 CNV with varying K values. B. (left) The number of SNVs specifically found from the population  
459 in Brazil and absent from all the other populations, counted from each individual in the invasive  
460 populations. (right) The number of SNVs specifically found from sfC-Florida and absent from all  
461 the other populations, counted from each individual from invasive populations. C. (left) The number  
462 of SNVs in each of individuals from Brazil that are not found from sfC-Florida. (right) The number  
463 of SNVs in each of individuals from sfC-Florida that are not found from Brazil. The error bars  
464 indicate 95% confidence intervals calculated from 1,000 times of bootstrapping replication in the  
465 way of resampling from 100kb windows.

466

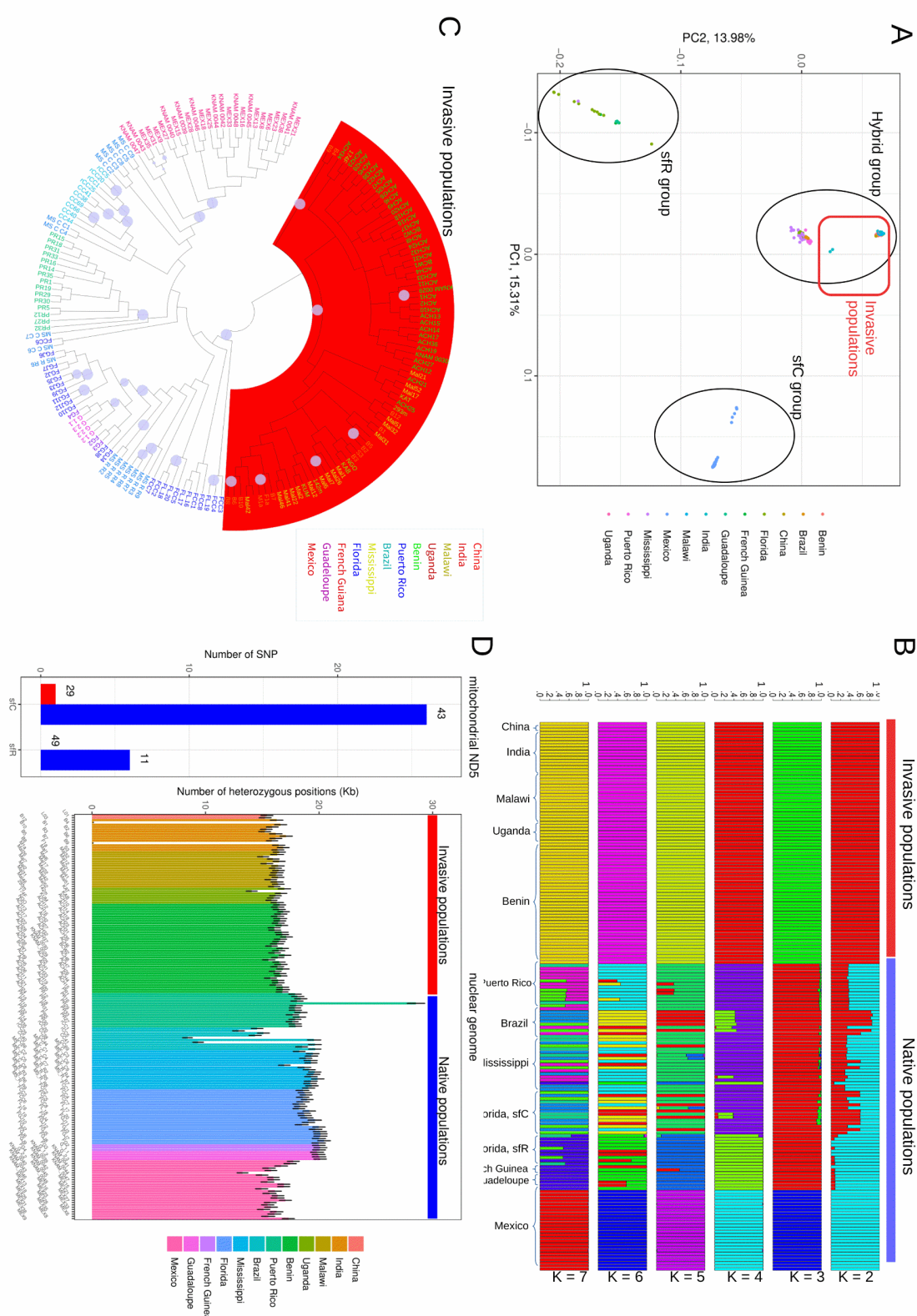
467 **Figure 3. Genomic balancing selection.** A. The LD decay curves calculated from each strain in  
468 each invasive population and their origins (sfC\_Brazil and sfC\_Florida). B. Correlation of  
469 nucleotide diversity between invasive populations and native hybrid population.

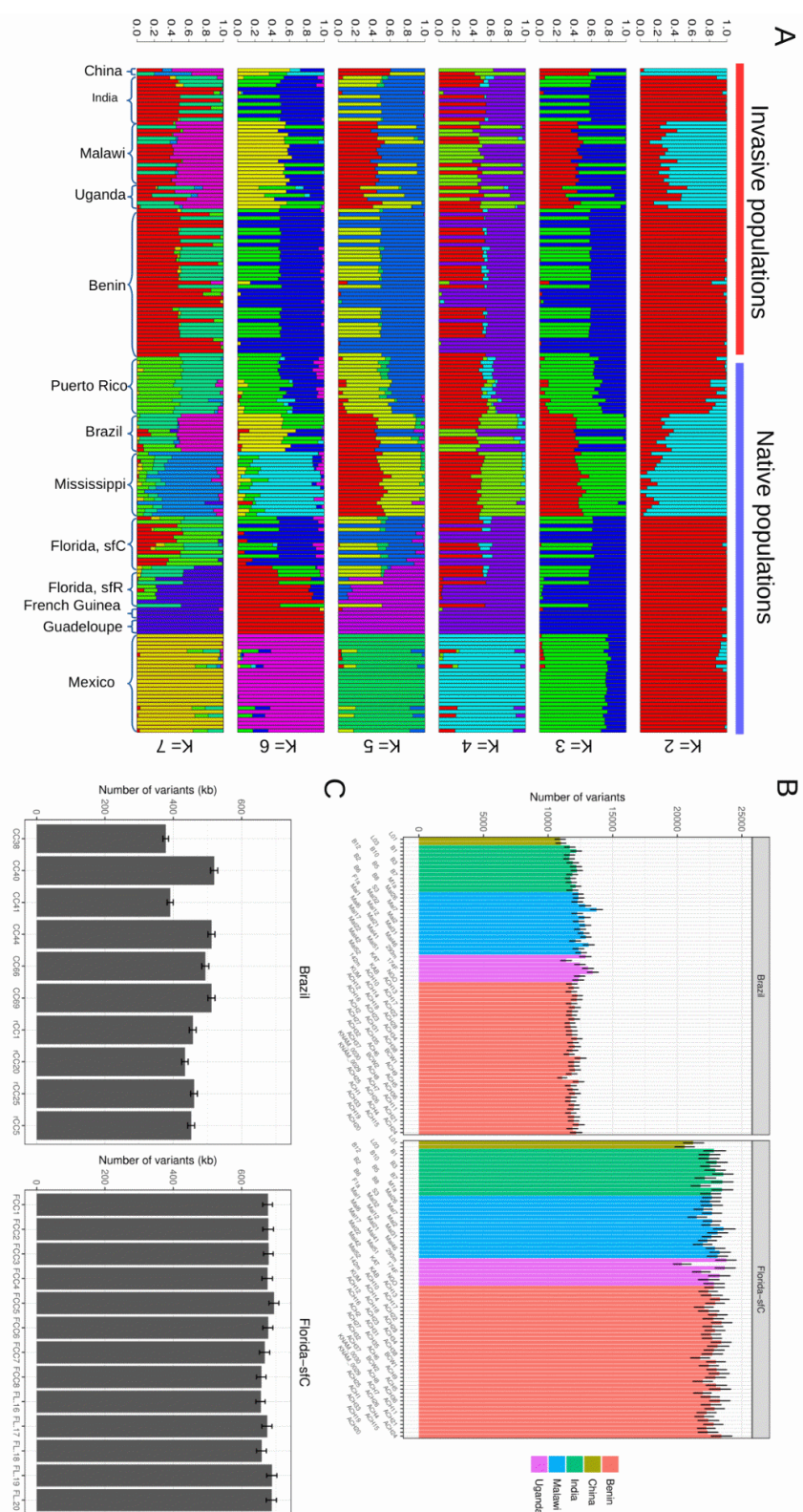
470

471 Figure 4. **Testing interspecific hybridization** A. Histogram of  $F_{ST}$  calculated from 100kb  
472 windows between invasive populations and native hybrid groups. The red vertical bar indicates  $F_{ST}$   
473 equals to zero. B. Homozygous variant positions were counted for each individual. The error bars  
474 indicate 95% confidence intervals calculated from 1,000 times of bootstrapping replication in the  
475 way of resampling from 100kb windows.

476

477 Figure 5. **Loci under positive selection** A. The composite likelihood of being targeted by selective  
478 sweeps in invasive populations. The red asterisks indicate invasive population-specific outliers of  
479 the composite likelihood ( $>100$ ), potentially targeted by selective sweeps. B.  $F_{ST}$  calculated from  
480 pairs of groups in CNV and SNV. The error bars indicate 95% confidence intervals calculated from  
481 1,000 times of bootstrapping replication in the way of resampling from 100kb windows. C. Allele  
482 frequency of the CNV locus containing the DDSS gene. CH0, CH1, and CH2 indicate zero, one,  
483 and two copies in a haploid genome, respectively.





486

